Tagawa *et al. J Wood Sci* (2019) 65:47
https://doi.org/10.1186/s10086-019-1826-0

Journal of Wood Science

ORIGINAL ARTICLE Open Access

Dynamics of structural polysaccharides deposition on the plasma-membrane surface of plant protoplasts during cell wall regeneration

Satomi Tagawa[1], Yusuke Yamagishi[2], Ugai Watanabe[3], Ryo Funada[4] and Tetsuo Kondo[1*]

Abstract

In this study, dynamic changes in structural polysaccharide deposition on the plasma membrane and cortical microtubules (CMTs) behavior were monitored in protoplasts isolated from white birch callus using confocal laser scanning microscopy and atomic force microscopy. We focused on the influence of an environmental stimulus on cell wall regeneration in protoplasts by employing an acidic culture medium containing a high concentration of Ca^{2+} (the stress condition). Under the non-stress condition, cellulose microfibrils and callose were initially synthesized, and thereafter deposited on the plasma membrane as "primary cell wall material". Under the stress condition, callose micro-sized fibers were secreted without cell wall regeneration. Behavior of CMTs labeled with mammalian microtubule-associated protein 4 with green fluorescent protein in transgenic protoplasts was monitored by time-lapse video analysis. Under the non-stress condition, CMTs behavior showed a linear arrangement at a fixed position, whereas unfixed manner of CMTs behavior was observed under the stress condition. These findings indicate that excessive Ca^{2+} affects cellulose synthesis and CMTs dynamics in plant protoplasts. Current study first demonstrated dynamics of cell wall regeneration and CMTs in woody protoplast, which provides novel insight to aid in understanding early stages of primary cell wall formation in plants.

Keywords: Plant protoplasts, Callose, Cell wall formation, Stress-response, Cortical microtubules

Introduction

The primary cell wall, which is a thinner membrane-type wall, is deposited on the cell surface during cell division and expansion. As the primary wall defines the final cell shape, it is considered to be a template for the following deposition of thick, dominant secondary cell walls. Studying the process of primary wall formation is indispensable for clarification of the early stages of cell wall formation in plants. Research on the structure of primary cell walls has been carried out mostly with a biochemical focus together with microscopic visualization. Early studies on primary cell wall structure began with isolation of cell walls and biochemical analyses of the component polymers, such as β1,4-glucan, β1,3-glucan, pectic polysaccharides, and xyloglucan [1, 2]. Subsequently, cell wall-related research employed transmission electron microscopy with immunocytochemical and enzyme-gold labeling techniques in addition to biochemical analyses, which were capable of visualizing the localization of specific molecules in the cell [3–5]. In addition, direct information on the three-dimensional molecular architecture of cell walls has been provided by transmission electron microscopy using shadowed replicas of rapidly frozen deep-etched specimens [6–8]. Recently, atomic force microscopy (AFM) has been used to characterize the nanoscale and mesoscale structure of primary cell walls in relation to mechanical properties [9, 10]. These results are statically investigated for already formed cell walls of

*Correspondence: tekondo@agr.kyushu-u.ac.jp
[1] Graduate School of Bioresource and Bioenvironmental Sciences, Kyushu University, West 5th, 744, Motooka, Nishi-Ku, Fukuoka 819-0395, Japan
Full list of author information is available at the end of the article

either primary or secondary cell walls. In situ dynamic investigation is required to understand the process of cell wall formation.

Cultured protoplast is one of the suitable materials to allow investigation of the dynamics of primary cell wall formation, e.g., arrangements of cellulose microfibrils and the sequence of polysaccharide synthesis, as well as compositional changes in cell walls during cell division [11–17]. Protoplasts, which lack cell walls, are appropriate for investigation of primary wall formation from initiation to the final stages. In addition, protoplasts are highly sensitive to the culture conditions and thus represent a suitable experimental system to monitor cell responses to environmental stresses.

Kondo et al. [18] investigated the effects of environmental stimuli on cell wall formation by a stressed protoplast culture under a severely modified Murashige and Skoog (MS) medium for *Betula platyphylla* (white birch) protoplasts prepared from the leaves [19–21]. A unique phenomenon was observed in the protoplasts, which was secretion of a bundle of callose hollow fibrils (=a callose hollow fiber) from a single site on the plasma-membrane surface in the presence of a high concentration of Ca^{2+} under an acidic pH [20, 21]. A similar phenomenon was observed in protoplasts of other woody plants [13, 22]. Moreover, Matsuo et al. [23] examined protoplasts from callus of white birch leaves and established a more efficient culture system to induce secretion of the callose hollow fibers. Recently, this phenomenon also has been reported in protoplasts of herbaceous plants [24].

Seyama and Kondo [21] reported that cell wall regeneration may be inhibited under the stress culture condition employed in the study. These authors examined the ability of cell wall regeneration in protoplasts culture under the stress condition by scoring the proportion of burst cells among protoplasts cultured under the stress condition for different durations and then exposed to low osmotic pressure. A high burst ratio was observed under the stress condition, regardless of the culture duration, which indicated that cell wall regeneration was inhibited. However, the mechanism for deposition of β-glucans on the cell surface, but not as a cell wall, under stress conditions remains unclear.

Previous reports have investigated cell wall formation by protoplasts of herbaceous plants [11, 14–17, 24], but few comparable studies have been undertaken on protoplasts of woody plants [12], which are important for biomass utilization. Therefore, the current study aimed to clarify the occurrence of cellulose microfibrils (CMFs) in protoplasts of white birch callus under the stress culture condition by in situ observation. The dynamics of CMTs, which play an important role in cell wall formation, and cell division was also examined by probing with mammalian microtubule-associated protein 4 (MAP4) fused with the green fluorescent protein (GFP-MAP4) [25]. As far as we know, this is the first report that demonstrated live cell imaging of CMTs in woody protoplasts. Cell wall regeneration may be regarded as a dynamic system influenced by environmental stimuli, and the present results provide a novel insight to aid in understanding cell wall formation and stress tolerance in woody plants.

Materials and methods

Materials

Callus induced from *Betula platyphylla* Sukatchev var. *japonica* Kan No. 8 was used for preparation of protoplasts [23]. The calli were subcultured every 3 weeks on Murashige and Skoog (MS) agar medium supplemented with 2 mM α-naphthalene acetic acid (NAA), 1 mM *N*-(2-chloro-4-pyridyl)-*N*′-phenylurea (4PU), and 1% (w/v) agar [18]. The cultures were incubated at 25 °C under visible light (3000–4000 lx) with a 16 h/8 h (light/dark) photoperiod.

Preparation of protoplasts

Protoplasts were prepared following a previously described procedure [23] with modifications. Calli cultured under the above-mentioned conditions for 2 weeks were transferred to a flask-containing MS liquid medium and shaken at 190 rpm to loosen the cell clusters. After 3–4 days, the protoplasts were isolated by treatment with 0.6 M mannitol solution containing 1% cellulase Onozuka R-S (Yakult Honsha Co., Ltd., Tokyo, Japan) and 1% Macerozyme R-10 (Yakult). Following the enzymatic treatment, the suspension was filtered through nylon mesh (pore size 40 × 40 μm^2) to obtain the protoplasts. After washing with 0.6 M mannitol, the protoplast precipitates were collected by centrifugation at 150*g* for 5 min. An appropriate volume of fresh 0.6 M mannitol solution was added prior to repeated centrifugation, and this treatment was repeated twice.

Protoplast culture

Culture of protoplast was started immediately after preparing the protoplasts. The protoplasts were cultured under stress (i) and non-stress (ii) conditions. The stress condition (i) was in accordance with that used by Matsuo et al. [23]: the prepared protoplasts were cultured in half-strength MS liquid medium supplemented with 1 mM NAA and 1 mM 4PU, and then, 150 mM $CaCl_2$ was added to the culture medium and the pH was adjusted to 3.5. The non-stress condition (ii) comprised half-strength MS liquid medium, supplemented with 1 mM NAA and 1 mM 4PU, with the addition of 0.6 M mannitol. The cell density was adjusted to

approximately 5×10^4 cells ml^{-1} in the culture well (equivalent to 2500 cells per well) prior to incubation at 28 °C in the dark. All protoplasts were cultured in 96-well microplates (Corning, Inc., NY, USA) and were directly observed under an inverted light microscope (CK40, Olympus Co., Tokyo, Japan).

Introduction of *GFP-MAP4* into calli as a fluorescent probe by *Agrobacterium tumefaciens*-mediated transformation

Microtubules were visualized by introduction of *GFP-MAP4* [25] into calli by the *Agrobacterium*-mediated transformation method [26]. The structure of the chimeric gene sequence is illustrated in Fig. 1. The disarmed strain *Agrobacterium tumefaciens* LBA4404 [27] that harbored a binary vector (pBI1101; Clontech Laboratories, Inc., Palo Alto, CA, USA) containing *GFP-MAP4* was used in the transformation experiments. *Agrobacterium tumefaciens* was cultured overnight at 28 °C in liquid yeast extract-mannitol medium in the presence of 50 mg l^{-1} kanamycin, and this culture was used for transformation of birch calli. The birch calli were incubated for 30 min in the diluted culture of *A. tumefaciens*, then incubated for 48 h on MS medium (pH 5.8) supplemented with 1% (w/v) agar and 100 μM acetosyringone (4-acetyl-2,6-dimethoxyphenol; Sigma-Aldrich Co. LLC, Tokyo, Japan). Each segment was washed five times with liquid MS medium. The calli were cultured on selective callus-induction medium [MS medium supplemented with 100 mg l^{-1} kanamycin, 500 mg l^{-1} carbenicillin, 2 mM NAA, 1 mM 4PU and 1% (w/v) agar]. After calli development for 2–3 months, the grown portions were transferred to fresh selective medium (MS medium supplemented with 50 mg l^{-1} kanamycin, 250 mg l^{-1} carbenicillin, 2 mM NAA, 1 mM 4PU, and 1% (w/v) agar). The grown portions then were transferred to normal (non-stress) medium. The transformed protoplasts were selected from the transformed calli by enzymatic treatment.

To confirm gene expression of GFP-MAP4, total RNA was extracted using an RNeasy Plant Mini kit (Qiagen, Inc., Hilden, German) from freezing calli, and first-strand cDNA was synthesized with ReverTra Ace reverse transcriptase (Toyobo, Co., Ltd., Osaka, Japan). *GFP-MAP4* was amplified by PCR using the primer pair of 5′-ATG GTGAGCAAGGGCGAG-3′ and 5′-ACCTCCTGCAGG AAAGTGGC-3′. PCR was performed under the standard condition of 30 cycles for the analysis of *GFP-MAP4* introduction line.

Confocal laser scanning microscopy

Protoplasts cultured under the non-stress and stress conditions were transferred to a glass-bottom 96-well dish (AGC Asahi Glass, Tokyo, Japan) for observation by confocal laser scanning microscopy (CLSM: Leica SP8; Leica Microsystems, Wetzlar, Germany). Prior to the incubation for more than 10 min, 10 μg ml^{-1} of Calcofluor white (CW; Sigma-Aldrich) for staining of β1,4-glucan (cellulose) and β1,3-glucan (callose) [28] and 10 μg l^{-1} of aniline blue fluorochrome (ABF; Biosupplies Australia, Pty. Ltd., Victoria, Australia) for specific staining of callose [29] were added separately to the culture. The pH was adjusted to approximately 6.0 [30] with 1% KOH solution with CW in the stress condition before CLSM observation.

Cellulase Onozuka R-S (Yakult) was used to investigate the degradability of products from protoplasts under CLSM to confirm the presence of cellulose. Protoplasts in the microplates were incubated with 0.1% cellulase Onozula R-S for 24 h at 28 °C in the dark. CLSM follows CW staining.

Substances deposited on protoplasts and microtubules linked to GFP-MAP4 were observed by CLSM. CW and ABF were excited at a wavelength of 405 nm in the irradiated beam using direct diode laser, and GFP-MAP4 was excited at 489 nm in the irradiated beam using white light laser with acousto-optic tunable filter. Fluorescence emission by CW and ABF was detected at 430–470 nm by hybrid detector, whereas GFP-MAP4 fluorescence was detected at 490–600 nm by hybrid detector (Leica Microsystems, Wetzlar, Germany). The fluorescence was collected by prism splitting system.

Atomic force microscopy

CMFs synthesized on the plasma membrane as a building block for cell walls were observed with an atomic force microscope (AFM). Samples for AFM were prepared in accordance with the modified method described previously [31]. Cultured protoplasts were fixed with 2.5% glutaraldehyde aqueous solution and then washed with 50 mM EDTA (pH 7.0). After fixation, the protoplasts were treated with 0.3% sodium dodecyl sulfate (SDS; Sigma-Aldrich) twice every 24 h to remove protein present on the cell surface. Aqueous urea (50%) was used to remove SDS twice every 12 h. Hemicellulose was removed by dissolution in 5% aqueous KOH solution twice every 24 h, and then, the protoplasts were washed with distilled water to remove the

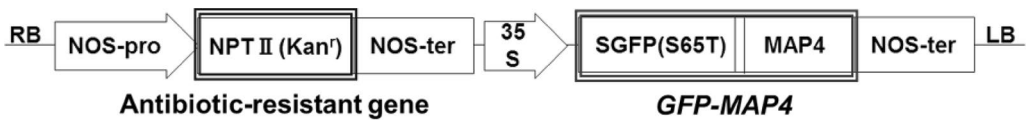

Fig. 1 Schematic diagram of GFP-MAP4 chimeric gene (modified from Marc et al. [25])

KOH solution. For observation, a droplet of the protoplast cultures was placed on a microscope glass slide and then air dried. Cellobiohydrolase I (CBH-I) from *Hypocrea jecorina* (Sigma-Aldrich) was used to investigate whether microfibrils on the plasma membrane were crystalline CMFs. The dried protoplasts were incubated in 1 U CBH-I aqueous solution for 24 h at 30 °C, and then washed with distilled water and air dried.

AFM micrographs of the surface of the dried protoplasts were acquired by an MFP-3D-SA AFM (Oxford Instruments Asylum Research, Inc., Santa Barbara, CA, USA) operated at room temperature, controlled in the non-contact mode with a scan rate 1.0 Hz to observe 1 μm^2 areas. An etched-silicon AFM tip was employed with a nominal radius of 7–11 nm and a spring (force) constant of 26 Nm^{-1}, which was shaped like a polygon-based pyramid with a height of about 14 μm and a cone angle of 35°. Scanning was carried out in both directions of the fiber axis and perpendicular to the axis. The width and height of the fiber aggregates were measured using a cross-sectional line profile analysis. The apparent width data (D) should include geometrical enhancement (E) depending on the radius (R) of the AFM tip. In the present observations, as the height of the aggregates was smaller than the radius of the tip, the following correction equation was employed [32]: $E = 2 \times (RH - H^2)^{1/2}$, $w = W - E$, where E is the geometrical enhancement on the real width value (w), W is the apparent width observed with the AFM, H is the height of the object observed with the AFM, and R is the AFM tip radius (7 nm).

Image analysis

CLSM micrograph image processing was performed using LAS X (Leica Microsystems, Wetzlar, Germany) and Image J/Fiji (W. Rasband, National Institutes of Health, Bethesda, MD, USA) software. Serial z-stack CLSM images were integrated into projection images using LAS X. The estimated proportion of coverage with cell walls for the entire protoplast surfaces was calculated using CLSM images based on the binarization and area fraction function of Image J/Fiji. Extension and shrinking velocity were calculated using CLSM images based on the tracking function of Image J/Fiji. The relative intensity of both CMTs and CW was calculated using CLSM images based on the plot profile function of Image J/Fiji.

Results and discussion

Inhibition of cell wall formation correlated with induced secretion of micro-sized fibers of callose under the stress condition

Light microscopic images of protoplasts cultured under the non-stress and stress conditions are compared in Fig. 2. Under the non-stress condition, the protoplasts enlarged and began to deform from spherical to elliptic–spherical in shape at 7 days. At culture for 14 days and 21 days, the protoplasts divided to form colonies (indicated by arrows in Fig. 2). Under the stress condition, however, protoplasts remained spherical in shape even after culture for 21 days, and cell division did not occur. Instead, the protoplast synthesized a micro-sized fiber (indicated by arrow head in Fig. 2).

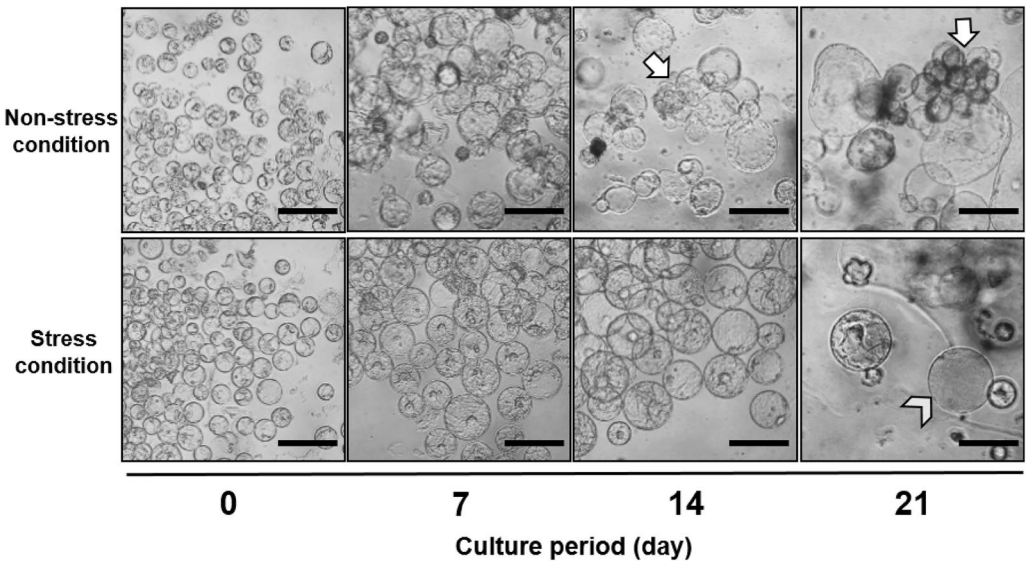

Fig. 2 Morphological changes of protoplasts. Light microscopic images of protoplasts at 0, 7, 14, and 21 days of culture under non-stress and stress conditions. Arrows indicate protoplast colonies. The arrow head indicates a protoplast secreting a micro-sized fiber. All scale bars = 100 μm

Seyama and Kondo [21] previously reported inhibition of cell wall formation by protoplasts under the present stress condition. However, cell wall regeneration had not been sufficiently investigated. During cell wall regeneration, two polysaccharides, cellulose and callose, are particularly important [33]. Cellulose (β1,4-glucan) is the most widely and commercially available polymer component in plant cell walls, constituting 30–90% of structural polysaccharides [34]. A unique cell wall polysaccharide component is callose (β1,3-glucan), which is specifically restricted to cell plates, pollen tubes, plasmodesmata, and wounded cells [34]. Thus, the presence of these two components during cell wall formation on protoplasts was the focus of CLSM in the current study under stress and non-stress culture conditions.

Under the non-stress condition, images of cellulose and callose stained with CW indicated the formation of aggregates on the protoplast surface within a few hours of initiation of the culture (0 day in Fig. 3). Apparent primary walls with a 'network structure' had already formed on the protoplasts after culture for 1 day (1 day in Fig. 3). At 7 days, networks of fibrils almost entirely covered the protoplasts (7 days in Fig. 3).

In contrast, under the stress condition, no fibril or network structure covered the protoplasts; instead, micro-sized fibers appeared (indicated by arrows in Fig. 3). Based on the images captured after culture for 14 days (data not shown), the percentage in coverage of products stained with CW on the cell surface was calculated as ca. 90% and ca. 30% for the non-stressed and stressed cultures, respectively. These results suggested that no cell wall deposition was observed for stress condition, while the cells under non-stress condition seem to regenerate cell wall.

Under the non-stress condition, inhomogeneous deposition of callose stained by ABF was observed on the cell surface (0, 1, and 7 days in Fig. 4). On the other hand, under the stress condition, twisted micro-sized fibers were apparent (arrows at 0, 1, and 7 days in Fig. 4), which corresponded with the appearance of substances stained with CW (Fig. 3).

Enzymatic degradation with cellulase can also be a useful tool to distinguish callose from cellulose. Under the non-stress condition, the substances covering the cells disappeared in response to the cellulase treatment (Additional file 1: Fig. S1a, b), whereas under the stress condition, the micro-sized fibers remained after enzymatic treatment (Arrows in Additional file 1: Fig. S1c, d). These results were consistent indicating that the micro-sized fibers comprised callose.

To investigate possible deposition of nanoscale CMFs, the surface of the protoplasts after culture for 14 days were observed by AFM. Before treatments with aqueous SDS and KOH, microfibrils were not apparent under both conditions (data not shown). After the treatments, however, microfibrils were visible under the non-stress condition, which indicated that the microfibrils were possibly covered with proteins, pectin, and hemicelluloses.

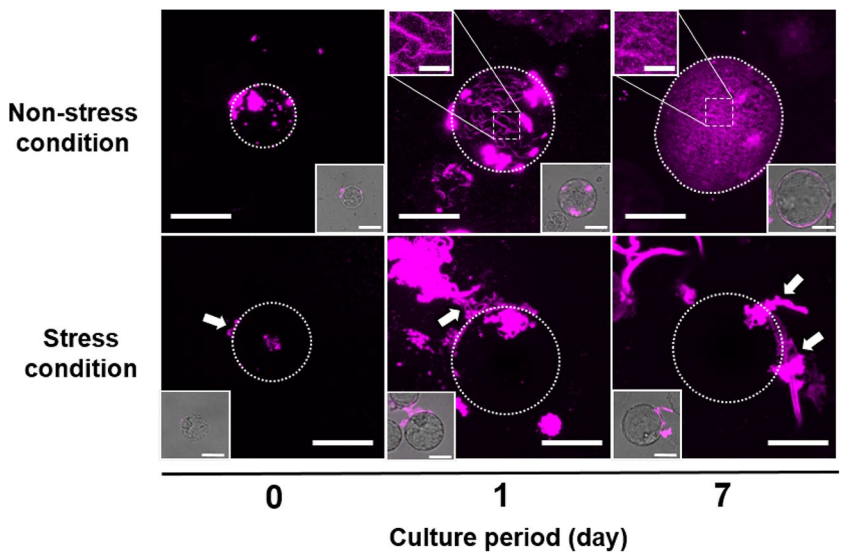

Fig. 3 Monitoring of deposition of cell wall components on the surface of protoplasts. CLSM projection images of CW fluorescence in protoplasts at 0, 1, and 7 days of culture under non-stress and stress conditions. Dashed lines indicate cell shape. Arrows indicate fibers secreted from protoplasts. Inset images indicate bright-field and CW fluorescence images of sections of protoplasts under the non-stress condition. Scale bars of main images = 25 µm; scale bars of inset images = 5 µm

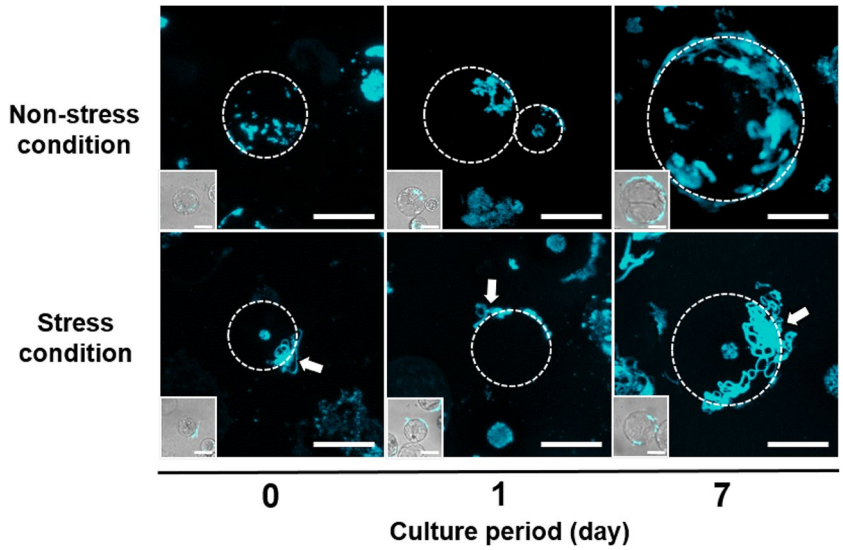

Fig. 4 Secretion of callose from protoplasts. CLSM images of ABF fluorescence in protoplasts at 0, 1, and 7 days of culture under the non-stress and stress conditions. Dashed lines indicate the cell shape. Arrows indicate micro-sized fibers secreted from protoplasts. Inset images indicate bright-field and CW fluorescence images of sections of protoplasts. All scale bars = 25 μm

Based on the tapping mode image (Fig. 5a, bottom), the size of the microfibrils was calculated as 2.9 ± 1.2 nm (mean ± SD, $n = 20$) in height and 25.7 ± 9.1 nm (mean ± SD, $n = 20$) in calibrated width. The deposited fibers were exhibited in a random orientation. As almost all the microfibrils disappeared after cellulase treatment (Additional file 1: Fig. S2), they were considered most likely to be CMFs. In contrast, under the stress condition, no microfibrils were detected on the protoplast surface (Fig. 5b), indicating no cellulose deposition on the protoplast surface under the stress condition.

Numerous investigations have indicated that the diameter of cellulose microfibrils in the range from 1.5 to 3.8 nm [35]. In the current study, the microfibril height was similar to the microfibril diameter, but the width was much larger. Taking into account the deviation tolerance range of the calibrated width, the microfibrils detected in the present study may have formed through coalescence of cellulose microfibrils, which would be ribbon-like CMFs.

The results presented in Figs. 2, 3, 4, and 5 indicate that fibril-like structures, including CMFs, were deposited on the plasma membrane under the non-stress condition (Fig. 3a). In contrast, the stress condition inhibited synthesis of CMFs. Specifically, the regeneration of cell wall, which is essential for cell division, did not occur under the stress condition. Therefore, comparison between the non-stress and stress conditions with regard to cell wall formation may provide crucial information on primary cell wall formation.

Callose was observed to form either in inhomogeneous depositions or in micro-sized fibers, depending on the non-stress and the stress culture conditions, respectively (Fig. 4). Some reports [36, 37] on cell wall formation indicate attachment of callose to deposited CMFs. Taking this into consideration, under the non-stress condition (Fig. 4) in the current study, callose might be located as inhomogeneous deposition on CMFs surrounding the plasma membrane. Namely, the presence of CMFs might inhibit fiber-like formation of callose in the non-stress condition.

Seyama et al. [20] reported that a low pH did not inhibit cell colony formation from protoplasts, which also indicates that a low pH does not inhibit cell wall formation. Thus, a high concentration of Ca^{2+} may be an important factor in the inhibition of cell wall formation or cellulose synthesis. Concerning Ca^{2+}, 1000-fold difference between cytoplasmic (100 nM) and non-cytoplasmic (mM) Ca^{2+} concentrations enables the generation of calcium signals by fast changes of cytoplasmic Ca^{2+} levels [38]. Therefore, excessive concentration of Ca^{2+} around cells possibly causes disturbance of calcium homeostasis. 150 mM of Ca^{2+} using in the current study might be regarded as an unusual environment for plant cells, resulting in inhibition of cell wall regeneration.

Cortical microtubules (CMTs) in protoplasts under the non-stress and stress conditions

Plant microtubules in cytoplasm are present beneath the plasma membrane to regulate the trajectory in

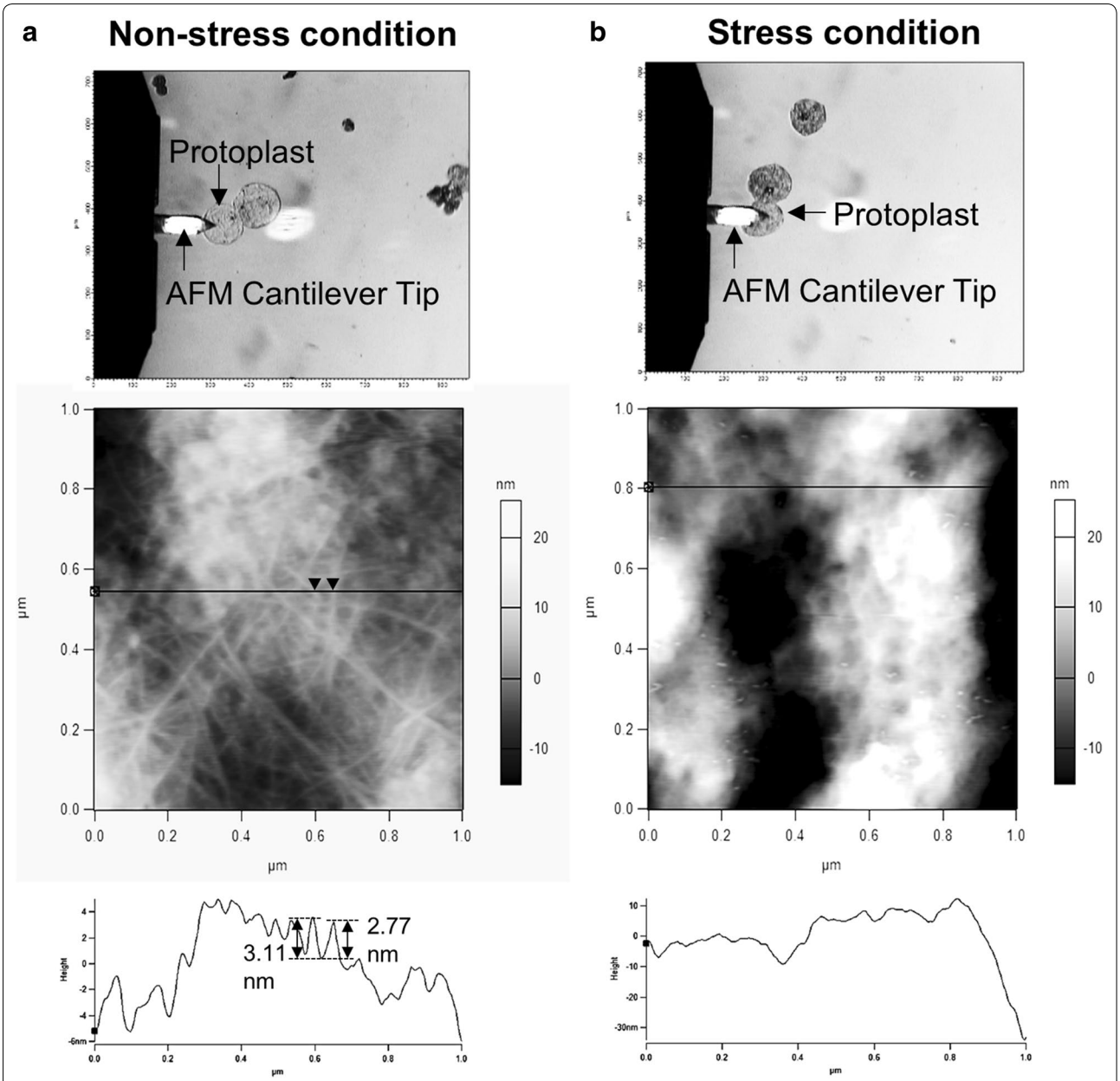

Fig. 5 Nano-surface of protoplasts. AFM images of the surface of protoplasts cultured under the non-stress (**a**) and stress (**b**) conditions at 14 days of culture after washing with 0.3% SDS and 5% KOH. Upper images indicate light microscopic images of protoplasts observed on AFM sample glass slides. Middle images correspond to AFM height images of tapping mode, and the graphs indicate the cross-section height along the horizontal line in the middle image. The arrow heads indicate the measured points of the height in the graph

movements of cellulose synthase complexes (CSCs) as a track [39, 40] via the cellulose synthase-interacting proteins [41, 42]. When CMTs are re-arranged, the moving trajectory of CSCs is immediately allowed to change [40, 43]. As mentioned in the previous section, cell wall formation and cell division were inhibited in the stress condition, which might be related to the dynamic behavior of CMTs. Therefore, in the present study, *GFP-MAP4* [25] was introduced into birch calli to provide GFP-MAP4 as a fluorescent probe attached to CMTs in isolated protoplasts. Due to the probe, the behavior of CMTs on the surface of protoplasts could be monitored by time-lapse video analyses using CLSM in relation to the culture condition.

Marc et al. [25] reported that GFP-MAP4 allows the constant monitoring of microtubule arrangements for

overextended periods of time when it was expressed at low levels, whereas at high levels, it induces an aberrant phenotype that is likely to inhibit normal microtubule function. Cells expressing high level of the transgene were unable to survive under mitotic conditions. Therefore, we select a callus line that constantly expresses the GFP-MAP4 gene by screening cultivation, which appears to grow and divided at a rate similar to that of non-gene modified callus.

Under the non-stress condition, the CMTs became linear and arrayed at many loci after 14 days of culture (Fig. 6a). Moreover, in the time-lapse analysis, movements of the CMTs exhibited repetition of both extension and contraction at a fixed position (indicated by arrows in Fig. 6a and Additional file 1: Fig. S3a), a well-known phenomenon "dynamic instability of the microtubules". In contrast, under the stress condition, the position of CMTs was not fixed, and they exhibited flexible displacement laterally (indicated by arrows in Fig. 6b). Dynamic instability of microtubules was still observed for the CMTs in the stressed cell (Additional file 1: Fig. S3b).

It has never been reported that excessive Ca^{2+} affects cellulose synthesis and CMTs' behavior in plant protoplasts. Elucidation of the reasons responsible for unfixed manner of CMTs is important to understand mechanisms of Ca^{2+} response and/or salt tolerance in plants.

CMFs following CMT arrays during cell wall regeneration

As described previously, CMTs behavior was supposed to correlate with the oriented deposition of CMFs on plasma membrane in plant cells. To confirm such a cooperated arrangement between CMFs and CMTs during cell wall regeneration in woody protoplasts, both of them were dual-visualized using fluorescent probes of CW and GFP-MAP4, respectively, in the cells cultured under non-stress conditions.

Under the non-stress condition at 3 day culture, CLSM observation for the dual-stained specimens exhibited some network of fibrils as cell wall components, which was confirmed as cellulose network in previous section, together with CMTs (Fig. 7). It is noted that the network of cellulose was not necessarily colocalized with CMTs. CW and GFP-MAP4 fluorescent image in the stress condition was no shown here, because synthesized polysaccharides stained with CW were not deposited on the plasma membrane as described for Fig. 3.

These results indicated that arrangement of CMTs possibly participated with arrangement of CMFs on plasma membrane. However, CMFs' position was fixed irrespective of dynamically moving CMTs, which may cause the mismatch of CMFs' and CMTs' positions. Similar results

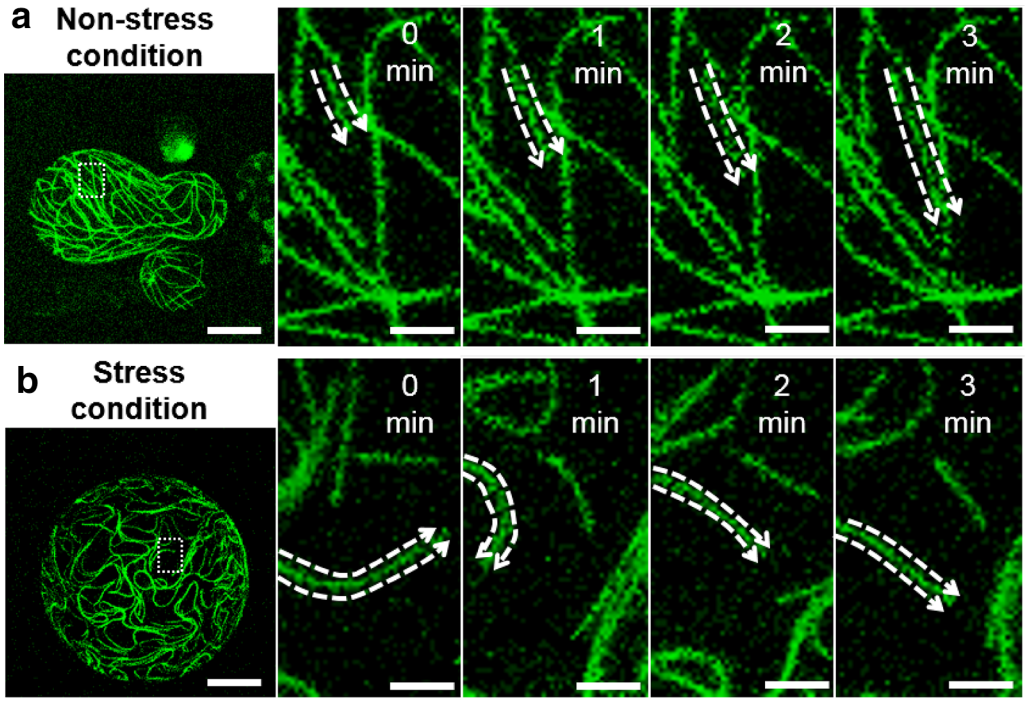

Fig. 6 Dynamics of CMTs' behavior labeled with GFP-MAP4 monitored by time-lapse video analyses. Successive CLSM projection images indicate movement of CMTs labeled with GFP-MAP4 under the non-stress (**a**) and stress (**b**) conditions at 27 days of culture. The left images provide an overview of CLSM projection images of the protoplasts. Scale bars = 25 μm. Dashed squares in the figures indicate magnified positions for the successive images. The interval of the individual image is 1 min each. Arrows indicate extension of the ends of microtubules. Scale bars = 4 μm

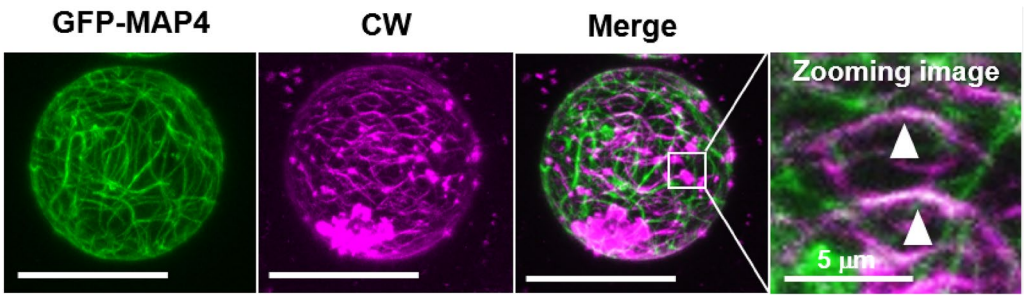

Fig. 7 Relationship between CMTs and cell wall components. Cell wall components (stained with CW) and CMTs (stained with GFP-MAP4) in protoplasts cultured under the non-stress condition at 3 days of culture. The arrow heads indicate colocalization of GFP-MAP4 and CW fluorescence. Scale bars = 25 μm

were reported by Kuki et al. [17] in *Arabidopsis* mesophyll protoplasts. Details of the relationship between CMTs dynamics and CMFs deposition in protoplasts under the stress and non-stress conditions will be investigated in future work.

Conclusion

The current study demonstrates dynamics of structural polysaccharides deposition relating to CMTs dynamics on the plasma-membrane surface of plant protoplasts during cell wall regeneration. Under the acidic stress condition, using a culture medium containing a high concentration of Ca^{2+}, cell wall regeneration was suppressed in protoplasts of white birch callus, which was possibly due to inhibition of CMFs deposition (Figs. 3, 5b). The absence of the cell wall might lead to formation of callose micro-sized fibers (Fig. 4). In contrast, under the non-stress condition, CMFs were deposited to establish cell walls (Figs. 3, 5a) and callose was deposited on the cell surface. The stress condition also affected CMT dynamics. Under the stress condition, CMTs behaved in an unfixed manner (Fig. 6b). The relationship with inhibition of CMF synthesis has been still unclear, but CMTs dynamics may be correlated with CMF deposition on the plasma membrane (Fig. 7). The simultaneous inhibition of CMF formation and the corresponding CMT dynamics were likely to be caused by the high concentration of Ca^{2+}.

Supplementary information

Supplementary information accompanies this paper at https://doi.org/10.1186/s10086-019-1826-0.

Additional file 1: Fig. S1. CLSM images of CW fluorescence in untreated (a, c) and cellulase-treated (b, d) protoplasts under non-stress condition (a, b) and stress condition (c, d). The arrows indicate callose hollow fibers. Scale bars = 200 μm. **Fig. S2.** Atomic force microscopic (AFM) amplitude-images of surfaces of protoplasts cultured under the non-stress condition before and after cellulase treatment. These images were taken at the same position of the surface of protoplast. **Fig. S3.** Successive confocal laser scanning microscopic (CLSM) projection images: These indicate movement of CMTs labeled with GFP-MAP4 under the non-stress (a) and stress (b) conditions at 27 days of culture. The interval of the individual image is 1 min each. The arrow heads indicate extension or contraction of the ends of CMTs. Scale bars = 4 μm.

Abbreviations

ABF: aniline blue fluorochrome; AFM: atomic force microscope; CBH-I: cellobiohydrolase I; CMTs: cortical microtubules; CMF: cellulose microfibril; CLSM: confocal laser scanning microscope; CW: Calcofluor white; CSC: cellulose synthase complex; 4PU: *N*-(2-chloro-4-pyridyl)-*N*′-phenylurea; GFP-MAP4: mammalian microtubule-associated protein 4 linked with green fluorescent protein; MS: Murashige and Skoog; NAA: α-naphthalene acetic acid; SDS: sodium dodecyl sulfate.

Acknowledgements

The authors are grateful to Center for Advanced Instrumental and Educational Supports, Faculty of Agriculture, Kyushu University for assistance in observation using CLSM (Leica SP8).

Authors' contributions

ST: mainly performed entire experiments and preparation of the paper; YY and UW: introduction of GFP into cortical microtubules; RF: discussion on the cell walls; TK: research plan through the study and preparation of the paper. All authors read and approved the final manuscript.

Funding

Not applicable.

Availability of data and materials

Not applicable.

Competing interests

The authors declare that they have no competing interests.

Author details

[1] Graduate School of Bioresource and Bioenvironmental Sciences, Kyushu University, West 5th, 744, Motooka, Nishi-Ku, Fukuoka 819-0395, Japan. [2] Research Faculty of Agriculture, Hokkaido University, 9 Kitakujonishi, Sapporo, Hokkaido 060-8589, Japan. [3] Faculty of Advanced Engineering, Chiba Institute of Technology, 2-17-1, Tsudanuma, Narashino, Chiba 275-0016, Japan. [4] Faculty of Agriculture, Tokyo University of Agriculture and Technology, Saiwaicho, Fuchu, Tokyo 183-8509, Japan.

Received: 24 January 2019 Accepted: 11 September 2019
Published online: 24 September 2019

References

1. Valent BS, Albersheim P (1974) The structure of plant cell walls: v. On the binding of xyloglucan to cellulose fibers. Plant Physiol 54:105–108
2. McNeil M, Darvill AG, Fry SC, Albersheim P (1984) Structure and function of the primary cell walls of plants. Annu Rev Biochem 53:625–663
3. Ruel K, Joseleau JP (1984) Use of enzyme-gold complexes for the ultrastructural localization of hemicelluloses in the plant cell wall. Histochemistry 81:573–580
4. Moore PJ, Darvill AG, Albersheim P, Staehelin AL (1986) Immunogold localization of xyloglucan and rhamnogalacturonan I in the cell walls of suspension-cultured sycamore cells. Plant Physiol 82:787–794
5. Benhamou N (1989) Cytochemical localization of β-(1→4)-D-glucans in plant and fungal cells using an exoglucanase-gold complex. Electron Microsc Rev 2:123–138
6. McCann MC (1990) Direct visualization of cross-links in the primary plant cell wall. J Cell Sci 96:323–334
7. Satiat-J B, Martin B, Hawes C (1992) Plant cell wall architecture is revealed by rapid-freezing and deep-etching. Protoplasma 167:33–42
8. Fujino T, Itoh T (2009) Changes in the three dimensional architecture of the cell wall during lignification of xylem cells in *Eucalyptus tereticornis*. Holzforschung 52:111–116
9. Yakubov GE, Bonilla MR, Chen H, Doblin MS, Bacic A, Gidley MJ, Stokes JR (2016) Mapping nano-scale mechanical heterogeneity of primary plant cell walls. J Exp Bot 67:2799–2816
10. Zhang T, Zheng Y, Cosgrove DJ (2016) Spatial organization of cellulose microfibrils and matrix polysaccharides in primary plant cell walls as imaged by multichannel atomic force microscopy. Plant J 85:179–192
11. Hirai N, Sonobe S, Hayashi T (1998) In situ synthesis of *β*-glucan microfibrils on tobacco plasma membrane sheets. PNAS 95:15102–15106
12. Suzuki K, Itoh T, Sasamoto H (1998) Cell wall architecture prerequisite for the cell division in the protoplasts of white poplar, *Populus alba* L. Plant Cell Physiol 39:632–638
13. Fukumoto T, Hayashi N, Sasamoto H (2005) Atomic force microscopy and laser confocal scanning microscopy analysis of callose fibers developed from protoplasts of embryogenic cells of a conifer. Planta 223:40–45
14. Kwon H-K, Yokoyama R, Nishitani K (2005) A proteomic approach to apoplastic proteins involved in cell wall regeneration in protoplasts of *Arabidopsis* suspension-cultured cells. Plant Cell Physiol 46:843–857
15. Wiszniewska A, Powowarczyk B (2014) Studies on cell wall regeneration in protoplast culture of legumes—the effect on organic medium additives on cell wall components. Czech J Genet Plant Breed 50:84–91
16. Yokoyama R, Kuki H, Kuroha T, Nishitani K (2016) *Arabidopsis* regenerating protoplast: a powerful model system for combining the proteomics of cell wall proteins and the visualization of cell wall dynamics. Proteomes 4:34
17. Kuki H, Higaki T, Yokoyama R, Kuroha T, Shinohara N, Hasezawa S, Nishitani K (2017) Quantitative confocal imaging method for analyzing cellulose dynamics during cell wall regeneration in *Arabidopsis* mesophyll protoplasts. Plant Direct 1:1–10
18. Murashige T, Skoog F (1962) A revised medium for rapid growth and bio assays with tobacco tissue cultures. Physl Plant 15:473–497
19. Kondo T, Maghoshi J, Abe H, Sasamoto H (2000) Method for producing of non cellulosic callose fibers from protoplasts and callose fiber. Japan Patent No. 3936522 (Application 3932000-3220419)
20. Seyama T, Kimura S, Sasamoto H, Abe H, Kondo T (2008) Spinning of a gigantic bundle of hollow fibrils by a spirally moving higher plant protoplast. Planta 227:1187–1197
21. Seyama T, Kondo T (2012) Morphological responses of *Betula* protoplasts in fiber spinning. Holzforschung 66:407–411
22. Sasamoto H, Ogita S, Hayashi N, Wakita Y, Yokota S, Yoshizawa N (2003) Development of novel elongated fiber-structure in protoplast cultures of *Betula platyphylia* and *Larix leptolepis*. Vitro Cell Dev Pl 39:223–228
23. Matsuo S, Takenaga A, Seyama T, Kondo T (2013) Secretion of a bundle of (1→3)-*β*-glucan hollow fibrils from protoplasts of callus suspension under a Ca^{2+}-rich and acidic stressed condition. Holzforschung 68:69–73
24. Tagawa S, Kondo T (2018) Secretion of a callose hollow fiber from herbaceous plant protoplasts induced by inhibition of cell wall formation. JWS 64:467–476
25. Marc J, Granger CL, Brincat J, Fisher DD, Kao T-h, McCubbin AG, Cyr RJ (1998) A GFP-MAP4 reporter gene for visualizing cortical microtubule rearrangements in living epidermal cells. Plant Cell 10:1927–1939
26. Mohri T, Mukai Y, Shinohara K (1997) *Agrobacterium tumefaciens*-mediated transformation of Japanese white birch (*Betula platyphylla* var. japonica). Plant Sci 127:53–60
27. Horsch RB, Fry JE, Hoffmann NL, Eichholtz D, Rogers SG, Fraley RT (1985) A simple and general method for transferring genes into plants. Science 227:1229–1231
28. Haigler CH, Brown RM, Benziman M (1980) Calcofluor white ST Alters the in vivo assembly of cellulose microfibrils. Science 210:903–906
29. Evans NA, Hoyne PA (1982) A fluorochrome from aniline blue: structure, synthesis and fluorescence properties. Aust J Chem 35:2571–2575
30. Roncero C, Durán A (1985) Effect of Calcofluor white and congo red on fungal cell wall morphogenesis: in vivo activation of chitin polymerization. J Bacteriol 163:1180–1185
31. Kataoka Y, Kondo T (1998) FT-IR microscopic analysis of changing cellulose crystalline structure during wood cell wall formation. Macromolecules 31:760–764
32. Kondo T, Nojiri M, Hishikawa Y, Togawa E, Romanovicz D, Brown MR (2002) Biodirected epitaxial nanodeposition of polymers on oriented macromolecular templates. PNAS 99:14008–14013
33. van Amstel TNM, Kengen HMP (1996) Callose deposition in the primary wall of suspension cells and regenerating protoplasts, and its relationship to patterned cellulose synthesis. Can J Bot 74:1040–1049
34. Lee K, Marcus SE, Knox PJ (2011) Cell wall biology: perspectives from cell wall imaging. Mol Plant 4:212–219
35. Krassig AH (1993) Cellulose: structure, accessibility and reactivity. Gordon and Breach Science, Yverdon
36. Eggert D, Naumann M, Reimer R, Voigt CA (2014) Nanoscale glucan polymer network causes pathogen resistance. Sci Rep 4:4159
37. Falter C, Zwikowics C, Eggert D, Blümke A, Naumann M, Wolff K, Ellinger D, Reimer R, Voigt CA (2015) Glucanocellulosic ethanol: the undiscovered biofuel potential in energy crops and marine biomass. Sci Rep 5:13722
38. Stael S, Wurzinger B, Mair A et al (2012) Plant organellar calcium signalling: an emerging field. J Exp Bot 63:1525–1542
39. Gutierrez R, Lindeboom JJ, Paredez AR, Emons AC, Ehrhardt DW (2009) *Arabidopsis* cortical microtubules position cellulose synthase delivery to the plasma membrane and interact with cellulose synthase trafficking compartments. Nat Cell Biol 11:797–806
40. Paredez AR, Somerville CR, Ehrhardt DW (2006) Visualization of cellulose synthase demonstrates functional association with microtubules. Science 312:1491–1495
41. Bringmann M, Li E, Sampathkumar A, Kocabek T, Hauser M-T, Persson S (2012) POM-POM2/cellulose synthase interacting1 is essential for the functional association of cellulose synthase and microtubules in *Arabidopsis*. Plant Cell Online 24:163–177
42. Li S, Lei L, Somerville CR, Gu Y (2012) Cellulose synthase interactive protein 1 (CSI1) links microtubules and cellulose synthase complexes. PNAS 109:185–190
43. Chan J, Crowell E, Eder M, Calder G, Bunnewell S, Findlay K, Vernhettes S, Höfte H, Lloyd C (2010) The rotation of cellulose synthase trajectories is microtubule dependent and influences the texture of epidermal cell walls in *Arabidopsis* hypocotyls. J Cell Sci 123:3490–3495

Publisher's Note